

Local-field and exchange-correlation effects in optical spectra of semiconductors

V. I. Gavrilenko* and F. Bechstedt

Friedrich-Schiller-Universität, Institut für Festkörpertheorie und Theoretische Optik, Max-Wien-Platz 1, 07743 Jena, Germany

(Received 16 August 1996)

The density-functional theory with *ab initio* pseudopotentials has been used to study the linear optical response of semiconductors. We present results for optical spectra where the effects of the macroscopic local-field and microscopic exchange-correlation interaction are included beyond diagonal and random-phase approximations. Quasiparticle corrections to the single-particle energies have been added in the polarization function. Numerical calculations are performed for the column-IV materials Si, SiC, and diamond as model substances. [S0163-1829(96)07944-1]

Highly accurate calculations of optical properties of semiconductors without using any empirical parameters are of continuous interest.¹⁻⁴ Most of the theoretical studies are based on the independent-particle approximation⁵ [often called the random-phase approximation (RPA)] and a first-principles description of the electronic and atomic structure in the framework of the density-functional theory (DFT) in the local-density approximation (LDA). The independent-quasiparticle (QP) approximation has been used in Refs. 1 and 6. First attempts^{1,2} were made to go beyond the RPA, considering exchange-correlation (XC) corrections. Local-field (LF) effects⁵ due to the atomic structure of the matter influence the resulting optical spectra. However, they have been studied in only a few papers.^{2,3} These papers supplement earlier studies in the field⁷⁻¹⁰ (and references therein), in which LF and excitonic effects have been discussed in the framework of the empirical-pseudopotential method (EPM) or expansions of the eigenfunctions in terms of localized orbitals. However, a clear and detailed picture is still missing.

In this paper we demonstrate the restrictions of the RPA widely used in condensed-matter theory for a quantitative analysis of optical spectra. In the framework of *ab initio* DFT beyond the RPA, we systematically studied the number of important contributions to the optical functions of semiconductors: the nonlocality of the velocity operator, and local fields as well as exchange-correlation effects. In addition, XC self-energy effects,^{4,11} i.e., quasiparticle shifts of the electron and hole DFT-LDA energies, are discussed. An interplay between the effects studied is discussed. As model substances the column-IV materials diamond (C), silicon (Si), and silicon carbide (SiC) are considered.

According to Adler and Wiser,⁵ the macroscopic dielectric function, that governs the optical properties of a crystal, may be directly related to the zeroth element of the inverse of the microscopic dielectric matrix $\varepsilon(\mathbf{q}+\mathbf{G}, \mathbf{q}+\mathbf{G}'; \omega)$, where \mathbf{q} denotes a vanishing wave vector, and \mathbf{G}, \mathbf{G}' represent elements of the reciprocal Bravais lattice of the crystal. The longitudinal macroscopic function is defined as

$$\varepsilon^M(\hat{\mathbf{q}}; \omega) = \lim_{\mathbf{q} \rightarrow 0} \frac{1}{\varepsilon^{-1}(\mathbf{q}+\mathbf{G}, \mathbf{q}+\mathbf{G}'; \omega)} \Big|_{\mathbf{G}=\mathbf{G}'=0}, \quad (1)$$

where $\hat{\mathbf{q}} = \mathbf{q}/|\mathbf{q}|$ represents the direction of \mathbf{q} . The zeroth element of the inverse dielectric matrix is influenced by the off-diagonal elements of the dielectric matrix, which are due to the lattice periodicity and generate ‘‘umklapp’’ processes in the dielectric response. They are generally referred to as ‘‘local-field effects.’’⁵ We define these LF effects more exactly as the discrepancy between $\varepsilon^M(\mathbf{q}; \omega)$ and the zeroth element of the dielectric matrix, $\lim_{\mathbf{q} \rightarrow 0} \varepsilon(\mathbf{q}, \mathbf{q}; \omega)$.

The microscopic dielectric matrix

$$\varepsilon(\mathbf{q}+\mathbf{G}, \mathbf{q}+\mathbf{G}'; \omega) = \delta_{\mathbf{G}\mathbf{G}'} - v(\mathbf{q}+\mathbf{G})P(\mathbf{q}+\mathbf{G}, \mathbf{q}+\mathbf{G}'; \omega), \quad (2)$$

with $v(\mathbf{q}+\mathbf{G}) = 4\pi e^2/|\mathbf{q}+\mathbf{G}|^2$, is directly related to the polarization function P of the system under consideration. It contains the irreducible diagrams of the proper part of the two-particle Green function. Neglecting XC corrections to the two-particle Green function, i.e., applying the independent-particle approximation, P has to be replaced by the polarization function P_0 of independent particles (or quasiparticles). If XC effects on the longitudinal response are not neglected, e.g., within the DFT or DFT-LDA, the polarization function P appears instead that of independent particles P_0 . It can be easily proved^{2,3} that the expression for interacting particles takes the form

$$P(\mathbf{q}+\mathbf{G}, \mathbf{q}+\mathbf{G}'; \omega) = \sum_{\mathbf{G}''} \Gamma(\mathbf{q}+\mathbf{G}, \mathbf{q}+\mathbf{G}''; \omega) \times P_0(\mathbf{q}+\mathbf{G}'', \mathbf{q}+\mathbf{G}'; \omega), \quad (3)$$

where the matrix Γ arises from the vertex function of the system. Its inverse matrix is directly related to a kernel K_{XC} that describes the XC effects in the two-particle function beyond the RPA. Within the DFT it may be represented in real space by $K_{XC} = \delta^2 E_{XC}/(\delta n \delta n')$ with the electron density n and the total XC energy E_{XC} . Within the DFT-LDA the kernel is local in real space and does not depend on the frequency. As a result, the reciprocal-space representation for K_{XC} is independent of \mathbf{q} and ω . It holds that $K_{XC}(\mathbf{q}+\mathbf{G}, \mathbf{q}+\mathbf{G}'; \omega) = K_{XC}(\mathbf{G}-\mathbf{G}')$.

The $\mathbf{q} \rightarrow 0$ limit of expression (1) is required to obtain the optical response functions. This limit has to be taken with care to keep the correct analytical properties of this function

and the underlying inverse dielectric matrix.¹² In the limit of vanishing wave vectors the macroscopic dielectric function (1) transforms into

$$\varepsilon^M(\mathbf{q};\omega) = \hat{\mathbf{q}} \cdot \hat{\varepsilon}^M(\omega) \cdot \hat{\mathbf{q}}, \quad (4)$$

where the macroscopic optical tensor¹² ($i, j = x, y, z$)

$$\begin{aligned} \varepsilon_{ij}^M(\omega) = & \varepsilon_{ij}(\omega) - \sum_{\mathbf{G}, \mathbf{G}' (\neq 0)} \frac{|\mathbf{G}|}{|\mathbf{G}'|} W_i(\mathbf{G};\omega) \\ & \times S^{-1}(\mathbf{G}, \mathbf{G}';\omega) W_j^*(\mathbf{G}';-\omega) \end{aligned} \quad (5)$$

is related to the corresponding microscopic one following from the zeroth element (“head”) of the dielectric matrix (2),

$$\begin{aligned} \varepsilon_{ij}(\omega) = & \delta_{ij} + \frac{16\pi e^2 \hbar^2}{V} \sum_{\mathbf{k}} \sum_{c,v} \frac{1}{[\varepsilon_c(\mathbf{k}) - \varepsilon_v(\mathbf{k})]} \\ & \times \frac{\langle c\mathbf{k}|v_i|v\mathbf{k}\rangle \langle v\mathbf{k}|v_j|c\mathbf{k}\rangle}{[\varepsilon_c(\mathbf{k}) - \varepsilon_v(\mathbf{k})]^2 - \hbar^2(\omega + i\eta)^2} \end{aligned} \quad (6)$$

and functions

$$W_j(\mathbf{G};\omega) = \frac{16\pi e^2 \hbar}{|\mathbf{G}|V} \sum_{\mathbf{k}} \sum_{c,v} \frac{\langle c\mathbf{k}|e^{i\mathbf{G}\cdot\mathbf{x}}|v\mathbf{k}\rangle \langle v\mathbf{k}|v_j|c\mathbf{k}\rangle}{[\varepsilon_c(\mathbf{k}) - \varepsilon_v(\mathbf{k})]^2 - \hbar^2(\omega + i\eta)^2} \quad (7)$$

arising from “wing” elements $\varepsilon(\mathbf{q}, \mathbf{G};\omega)$. Here matrix elements of the velocity operator \mathbf{v} and exponential functions with the Bloch eigenfunctions $|n\mathbf{k}\rangle$ belonging to the band index n , the wave vector \mathbf{k} from the Brillouin zone (BZ), and the single-particle energy $\varepsilon_n(\mathbf{k})$ are introduced. S^{-1} is the inverse of the lower-right submatrix of $\varepsilon(\mathbf{q} + \mathbf{G}, \mathbf{q} + \mathbf{G}';\omega)$, corresponding to nonzero reciprocal-lattice vectors \mathbf{G} and $\mathbf{G}' \neq 0$, the so-called “body” of the dielectric matrix.

The electronic-structure calculations underlying the computations of the optical properties are based on the DFT-LDA.¹³ The electron-ion interaction is treated by norm-conserving, *ab initio*, fully separable pseudopotentials in the Kleinman-Bylander form. As model systems we consider silicon- and carbon-based crystals. The C potentials are softened by careful choosing of the core radii.¹⁴ The electronic wave functions are expanded in terms of plane waves. The energy cutoffs for the plane-wave expansion are chosen to 15, 34, and 42 Ry for silicon, silicon carbide, and diamond. The total-energy optimizations give rise to theoretical cubic lattice constants of $a = 10.227$ a.u. for Si, $a = 8.109$ a.u. for SiC, and $a = 6.681$ a.u. for C. We also study the influence of many-body QP effects. Thereby we overcome the scissors-operator approximation. The QP corrections to the DFT-LDA eigenvalues are computed within the GW approximation for the XC self-energy¹¹ according to a simplified scheme developed by Menzien *et al.*¹⁵ Using the numerical input described above corresponding shift values have been published for Si and diamond in Ref. 4, and for SiC in Ref. 15.

A crucial point of the calculations concerns the number of conduction bands N_{CB} and the rank $N_{\mathbf{G}}$ of the microscopic dielectric matrix taken into account. The convergence properties of the head, wing, and body elements with increasing N_{CB} are rather different. This holds also for the size of the

dielectric matrix that has to be inverted. The maximum matrix size considered is $N_{\mathbf{G}} = 89$. We conclude that a reasonable convergence is already obtained for a restriction up to \mathbf{G} vectors of type (222), independently of the inclusion of the XC kernel in addition to the LF effects or not. The rank of the matrix in this case is $N_{\mathbf{G}} = 59$. The sufficient number N_{CB} of conduction bands depends on the reciprocal-lattice vectors \mathbf{G} included in the dielectric matrix. In the computations of the frequency dependences we use the number $N_{\text{CB}} = 176$, which obviously gives converged results.

A crucial point of the explicit numerical calculations of the macroscopic dielectric function concerns the BZ integration. It should be reduced to the smallest possible part, for instance to the irreducible part of the BZ (IBZ). This is in general not possible. Since the matrix $\varepsilon(\mathbf{q} + \mathbf{G}, \mathbf{q} + \mathbf{G}';\omega)$ has the symmetry of the little group $G_{\mathbf{q}}$ of the wave vector \mathbf{q} , the degree of the BZ-integration reduction depends on \mathbf{q} . To achieve maximum computational efficiency we make full use of the symmetry under consideration. In the cubic case, the tensor $\varepsilon_{ij}^M(\omega)$ in Eq. (5) should be diagonal, $\varepsilon_{ij}^M(\omega) = \varepsilon^M(\omega) \delta_{ij}$, for symmetry reasons. Then the longitudinal dielectric function is indeed independent of the direction of \mathbf{q} . Therefore, only one diagonal component has to be calculated integrating in \mathbf{k} space over a part of the BZ larger than the IBZ. However, we consider the trace of the tensor to obtain the macroscopic dielectric function, $\varepsilon^M(\omega) = \frac{1}{3} \text{Tr}\{\varepsilon_{ij}^M(\omega)\} = \frac{1}{3}[\varepsilon_{xx}^M(\omega) + \varepsilon_{yy}^M(\omega) + \varepsilon_{zz}^M(\omega)]$. The trace is an invariant with respect to all point-group operations. Because of the invariance property of the trace the BZ integration of each diagonal element of the microscopic tensor can be reduced to the IBZ. The body of the dielectric matrix $\varepsilon(\mathbf{G}, \mathbf{G}';\omega)$, with $\mathbf{G}, \mathbf{G}' \neq 0$, has the symmetry of the Γ point, i.e., of the full point group. The corresponding matrix elements are therefore computed with the reduction of the BZ integration to the IBZ applying the method of invariants.

Critical points of the IBZ integration concern the density of the \mathbf{k} -point mesh and the type of integration. It has been proved previously that, in the calculation of the static dielectric constant, good convergence is achieved by the use of a relatively small number $N_{\mathbf{k}}$ of special \mathbf{k} points (see Ref. 11 and references therein). Typical numbers of $N_{\mathbf{k}}$ used were not very much larger than 10. However, calculating the whole spectra of $\text{Re}\varepsilon^M(\omega)$ and $\text{Im}\varepsilon^M(\omega)$ many more points are needed. We therefore apply a combination of the linear-tetrahedron method and a special-point technique for the \mathbf{k} -space integration. The most important diagonal head contributions $\varepsilon_{jj}(\omega)$ are calculated within the tetrahedron method with $N_{\mathbf{k}} = 89$. For the wing and body elements we use 235 special- \mathbf{k} points within the IBZ. To smooth the resulting spectra a Lorentzian broadening of $\eta = 0.1$ eV [cf. expressions (6) and (7)] is introduced.

Imaginary parts of the macroscopic dielectric functions resulting for C, SiC, and Si are plotted versus photon energy in Fig. 1 within different approximations: without LF and XC effects, with LF effects, with LF and XC effects, and with LF and XC effects but using QP eigenvalues instead of DFT-LDA ones. Changes of LF contributions due to inclusion of the XC kernel are plotted separately. The nonlocality, LF, and many-body XC effects have practically no influence on the peak positions, but give rise to remarkable renormal-

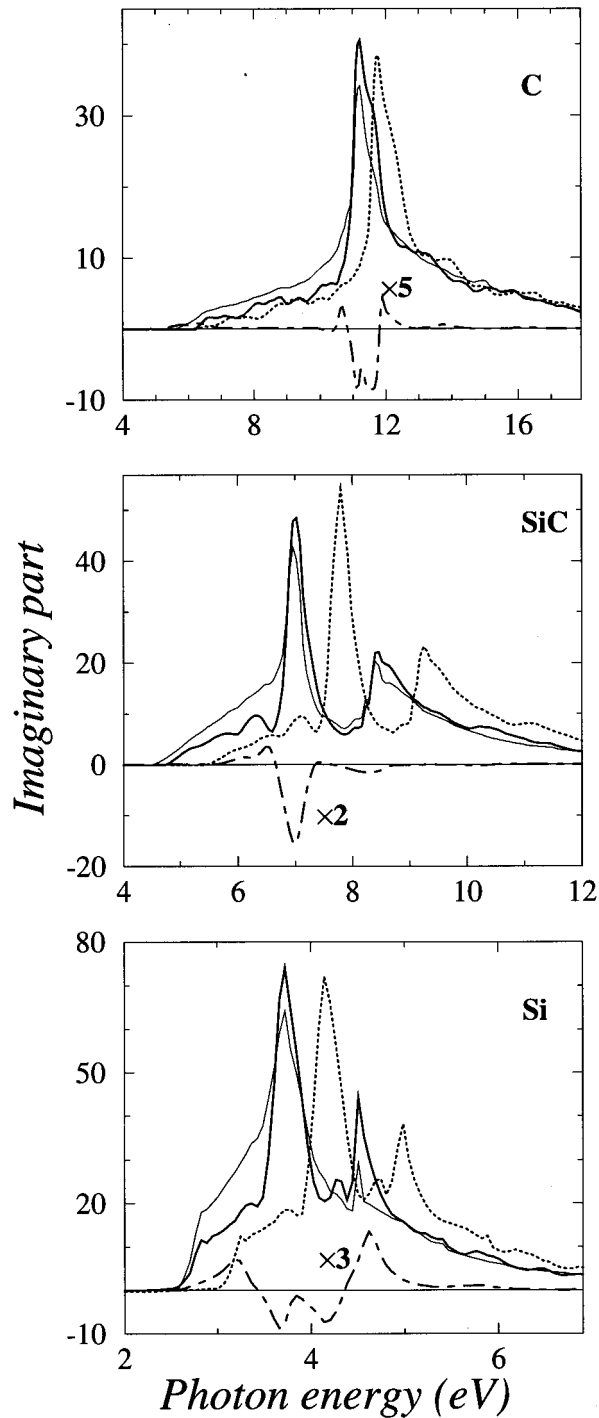


FIG. 1. Imaginary part of the macroscopic dielectric function of diamond, silicon carbide, and silicon vs photon energy. Thin solid line: without LF and XC effects (only $\mathbf{G}=\mathbf{G}'=0$ element); bold solid line: with LF and XC effects; dotted line: with LF and XC effects but shifted by wave-vector- and band-index-dependent QP corrections; dashed-dotted line: change of LF contribution due to inclusion of XC kernel in expression (3).

izations of the oscillator strengths. Compared with the $\mathbf{G}=\mathbf{G}'=0$ element of the dielectric function, the LF effects reduce the oscillator strength of $\varepsilon^M(\omega)$ in the spectral region below the main absorption peaks. On the other hand, the inclusion of the XC kernel reduces the LF effects in this region. The corresponding curves lie in between those for

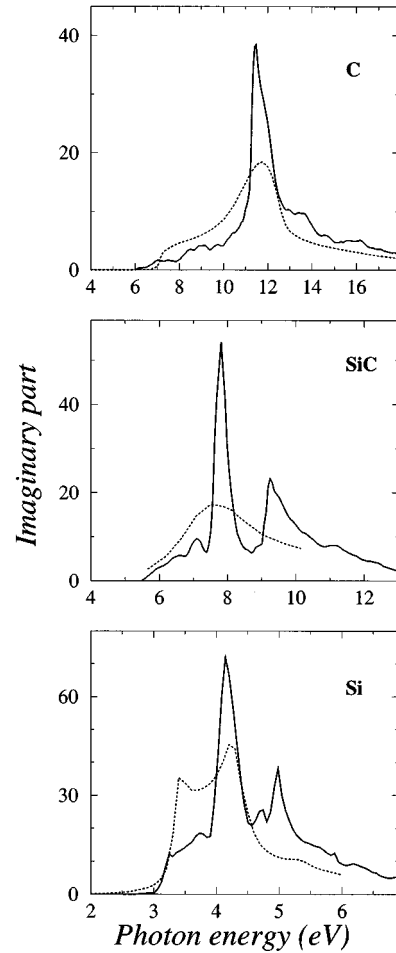


FIG. 2. Imaginary part of the macroscopic dielectric function of diamond, silicon carbide, and silicon vs photon energy. Solid lines: calculated results including LF, XC, and QP effects; dotted lines: experimental results for Si (Ref. 16), SiC (Ref. 17), and diamond (Ref. 18).

$\varepsilon(\omega)$ and $\varepsilon^M(\omega)$ including only LF effects. The net effect which incorporates LF and XC amounts to roughly 60% of the pure LF influence using the RPA expression for the polarization function. In the region of the main absorption peaks and above them, the situation is not unique. Positive and negative variations of the oscillator strengths occur. However, the strongest theoretical absorption peaks, i.e., E_2 for C and Si, E_o , E_1 , E'_o and E'_1 for SiC, and E'_1 for Si are increased by LF but somewhat reduced by XC effects. In the high-energy region above these peaks local fields slightly enhance the response whenever the XC effect in this region is negligible. The comparison of the spectra for C, SiC, and Si make it evident that LF and XC effects show only weakly pronounced chemical trends with the averaged size of the atoms, the localization of the wave functions, or the averaged density of the electrons. The strongest LF and XC effects appear for silicon whereas their relative influence is slightly reduced changing to diamond. This result is in agreement with earlier semiempirical calculations for Si and C.^{7,8}

In Fig. 2 the macroscopic dielectric functions of C, SiC, and Si are calculated within the DFT-LDA, but including LF, XC, and QP effects, and are compared with experimental

data.^{16–18} The theoretical spectra are shifted toward lower energies to bring the zeros of the experimental and theoretical real part together. For this purpose the calculated QP shifts $\Delta_n(\mathbf{k})$ are replaced by $A\Delta_n(\mathbf{k})$ with scaling factors $A=0.2$ (C), 0.45 (SiC), and 0.5 (Si). This scaling reduces the effect of the wave-vector- and band-index-dependent quasiparticle shifts calculated for Si, SiC, and C.^{4,15} Considering the comparison of theoretical and experimental optical spectra over a wide range of photon energies, one can conclude that the QP effect is overestimated for the most pronounced optical transition, e.g., E_1 and E_2 in Si and C, in contrast to electron-hole pair excitations near the fundamental indirect energy gap. As a consequence the scaling factors $A < 1$ have been introduced. Using the positions of the zero in the real parts of the macroscopic dielectric function in order to define averaged scissors operators Δ , from the wave-vector- and band-index-dependent QP corrections one derives values $\Delta=0.95$ (Si), 1.65 (SiC), and 2.65 eV (C). However, averaged scissors operators being necessary for a correct description of spectral positions only amount to $\Delta=0.47$ (Si), 0.84 (SiC), and $\Delta=0.40$ eV (C). The reason for this observation is not very clear. One possible reason could be related to excitonic effects which increase with the localization of the electronic states in the considered material. We mention that similarly small scissors operators have been found to bring the calculations of ϵ_∞ into agreement with experiment.¹ Conversely, the partial inclusion of QP effects shifts the theoretical peaks toward the position of experimental ones.

A general feature of the theoretical spectra for the imaginary parts of C and Si is that the overestimation of the intensity of the E_2 peak, i.e., the high-energy peak in $\text{Im } \epsilon^M(\omega)$, is further increased by the LF effects. However, the shoulder at the low-energy side of the theoretical spectra $\text{Im } \epsilon^M(\omega)$ is not enhanced but further reduced. These findings,

that LF effects shift the strengths of the $\text{Im } \epsilon^M(\omega)$ to high energies, are in agreement with the EPM calculations of Van Vechten and Martin,⁷ but these results are in conflict with the findings of Louie, Chelikowsky, and Cohen.⁸ We speculate that only the inclusion of the Coulomb attraction between the electron and hole can drastically redistribute the oscillator strengths from higher to lower photon energies.

In conclusion, we studied the influence of the number of important effects on the optical functions of semiconductors beyond the RPA. The influence of the nonlocality of the velocity operator, local-field effects, and exchange-correlation corrections on the optical properties of column-IV materials are studied in the framework of an *ab initio* density-functional method. We find that (i) these effects do not shift the prominent peak positions in $\text{Im } \epsilon^M(\omega)$, and that (ii) the agreement of theory and experiment remains still insufficient after inclusion of these effects. We found a weakly pronounced chemical trend. With rising electron localization, the influence of LF and XC decreases slightly. The influence of quasiparticle corrections is also checked, taking into account wave-vector- and band-index-dependent self-energy shifts. We observe an obvious remarkable overestimation of these shifts. In order to bring theoretical absorption spectra closer together with measured line shapes we suggest that excitonic effects have to be also included in the *ab initio* calculations. Our results show the restrictions of the RPA for a quantitative analysis of optical properties, and the necessity of including many-body effects into the theory.

This work was financially supported by the Deutsche Forschungsgemeinschaft (SFB 196, Projects Nos. A8 and B7) and the EC Programme Human Capital and Mobility (Contract No. ERBCHRXCT 930337).

*Present address: Physics Department, Brooklyn College of CUNY, 2900 Bedford Avenue, Brooklyn, New York 11210.

¹Z. H. Levine and D. C. Allan, Phys. Rev. Lett. **63**, 1719 (1989); Phys. Rev. B **43**, 4187 (1991); **42**, 3567 (1990); **44**, 12781 (1991).

²B. Engel and F. Farid, Phys. Rev. B **46**, 15 812 (1992).

³R. Daling, W. van Haeringen, and B. Farid, Phys. Rev. B **45**, 8970 (1992).

⁴B. Adolph, V. I. Gavrilenko, K. Tenelsen, F. Bechstedt, and R. Del Sole, Phys. Rev. B **53**, 9797 (1996).

⁵S.L. Adler, Phys. Rev. **126**, 413 (1962); N. Wiser, *ibid.* **129**, 62 (1963).

⁶R. Del Sole and R. Girlanda, Phys. Rev. B **48**, 11 789 (1993).

⁷J. A. Van Vechten and R. M. Martin, Phys. Rev. Lett. **28**, 446 (1972).

⁸S.G. Louie, J. R. Chelikowsky, and M. L. Cohen, Phys. Rev. Lett. **34**, 155 (1975).

⁹W. Hanke and L. J. Sham, Phys. Rev. B **21**, 4656 (1980); W.

Hanke, Adv. Phys. **27**, 287 (1978).

¹⁰H. Bross, O. Belhachemi, B. Mekki, and A. Seoud, J. Phys. Condens. Matter **2**, 3919 (1990).

¹¹M. S. Hybertsen and S. G. Louie, Phys. Rev. B **34**, 5390 (1986).

¹²R.M. Pick, M. H. Cohen, and R. M. Martin, Phys. Rev. B **1**, 910 (1970).

¹³R. Stumpf and M. Scheffler, Comput. Phys. Commun. **79**, 447 (1994).

¹⁴P. Käckell, B. Wenzien, and F. Bechstedt, Phys. Rev. B **50**, 17 037 (1994).

¹⁵B. Wenzien, P. Käckell, F. Bechstedt, and G. Cappellini, Phys. Rev. B **52**, 10 897 (1995).

¹⁶D. E. Aspnes and A. A. Studna, Phys. Rev. B **27**, 985 (1983).

¹⁷S. Logothetidis, H. M. Polatoglou, J. Petalas, D. Fuchs, and R. L. Johnson, Physica B **185**, 389 (1993).

¹⁸A. D. Papadopoulos and E. Anastassakis, Phys. Rev. B **43**, 5090 (1991).